Materials Transactions, Vol. 47, No. 11 (2006) pp. 2842 to 2845

Amorphous Formation and Magnetic Properties of Nd-Fe-Co-Al Alloys by Gas Flow Type Levitation Process

Shuji Azumo[1,*] and Katsuhisa Nagayama[1]

[1]*Department of Materials Science, Faculty of Engineering, Shibaura Institute of Technology, Tokyo 135-8548*

It is reported that Nd-Fe-Co-Al amorphous alloys have high bulk amorphous formation ability and high coercivity by rapid solidification method. We have examined the undercooling solidification, bulk amorphous formation and high coercivity appearance by using containerless process. In this study, we investigated the undercooling, bulk amorphous formation and magnetic properties for Nd-Fe-Co-Al alloys which are levitated and solidified by using the gas jet flow and high cooling type electromagnetic levitation system. Therefore, the high undercooling degree was 66–152 K and the samples formed amorphous phase. The bulk samples, ϕ6 mm sphere, solidified at the cooling rate, about 100 K/s. In addition, the coercivity for $Nd_{65}Fe_{10}Co_{15}Al_{10}$ sample with bulk amorphous phase, 3.7 kOe, was the highest value in all samples. Also, the thermal stability for $Nd_{65}Fe_{10}Co_{15}Al_{10}$ sample was carried out by isothermal annealing experiments. The origin of high coercivity may be related to the amorphous phase. [doi:10.2320/matertrans.47.2842]

(Received April 17, 2006; Accepted September 25, 2006; Published November 15, 2006)

Keywords: *containerless process, gas jet flow type levitation, neodymium-iron-cobalt-aluminum alloys, bulk amorphous phase, high coercivity*

1. Introduction

Nd-Fe-Al and Nd-Fe-Co-Al amorphous alloys have been reported to exhibit the hard magnetic properties and high glass-forming ability.[1–7] Nd-Fe-Al amorphous alloy with a diameter up to 12 mm has been recently prepared and has hard magnetic properties at room temperature.[8] Also, the containerless process is expected to form bulk metallic glass by the utility of high undercooling because it minimizes the chances of sample surface contamination. However, the electromagnetic levitation gives heating at the cooling period due to levitating and heating by the electromagnetic power. So, the cooling rate of electromagnetic levitation is slow (20–60 K/s). Therefore, the new containerless process has been developed by embedding the gas jet flow[9] or superconducting magnets.[10,11] By the above-described method, the heating at the cooling period is avoided and the samples can be solidified at the high cooling rate. Also, when samples were solidified, electromagnetic convection at the solidification can be avoided. The gas flow type levitating system has the simple apparatus configuration and gives the levitating and cooling of sample by gas jet flow. The electromagnetic power is used for only heating of samples. The cooling rate is 60–200 K/s then. By using this process, we have reported about the amorphous formation ability, magnetic properties and effect of Co addition of $Nd_{60}Fe_xCo_{30-x}Al_{10}$ alloys ($x = 0$, 10, 15 and 20).[7] However, the effect of amount of Nd hasn't been reported.

This paper presents amorphous phase formation and magnetic properties of Nd-Fe-Co-Al alloys with different amount of Nd by the gas flow type electromagnetic levitation.

2. Experimental

Ingots with composition of $Nd_{55}Fe_xCo_{35-x}Al_{10}$, $Nd_{60}Fe_xCo_{30-x}Al_{10}$ and $Nd_{65}Fe_xCo_{25-x}Al_{10}$ ($x = 0$, 10, 15 and 20) were prepared by arc metling from elemental Nd, Fe, Co and Al with a purity of 99.9% in argon atmosphere. From these ingots, the spheres with 6 mm in diameter were fabricated for levitation.

The furnace chamber was evacuated to 10^{-3} Pa by a turbo molecular pump and then filled with argon gas. The spherical sample was levitated and solidified by helium gas jet flow in quartz holder. Then, the electromagnetic power with 10 kW supply was used for the melting of spherical samples. The details of levitation method can be seen in Refs. 7) and 9). The temperature of the levitated sample was measured by two color pyrometer with Si and InGaAs as detecting component to examine solidification behavior with undercooling in these alloys.

The structure of the solidified samples was examined by X-ray diffractometer (XRD) using CuKα radiation at room temperature. The differential thermal analysis (DTA) of samples was carried out to identify an amorphous phase and determined the crystallization temperature, T_x, and the glass transition temperature, T_g, with a heating rate of 0.33 K/s. The magnetic properties of the solidified sample were measured by the vibrating sample magnetometer (VSM) at room temperature. The temperature dependence of magnetization for samples was measured at a maximum applied field of 500 Oe. The Curie temperature T_c was defined as the point of intersection between the linearly extrapolated curves of ferromagnetic and paramagnetic temperature region in this study.

3. Results and Discussion

3.1 Undercooling solidification

Figure 1 shows the typical cooling curves for the solidified $Nd_{65}Fe_xCo_{25-x}Al_{10}$ ($x = 0$, 10, 15 and 25) samples in the containerless state. The samples were solidified by helium gas flow rate with 10 L/min when the high frequency power was shut down. Also, a levitated sample was kept from the levitating start to the termination of solidification in stable condition. The average of the primary solidification cooling rate and the average cooling rate (cooling rate from cooling

*Graduate Student, Shibaura Institute of Technology, Tokyo 135-8548

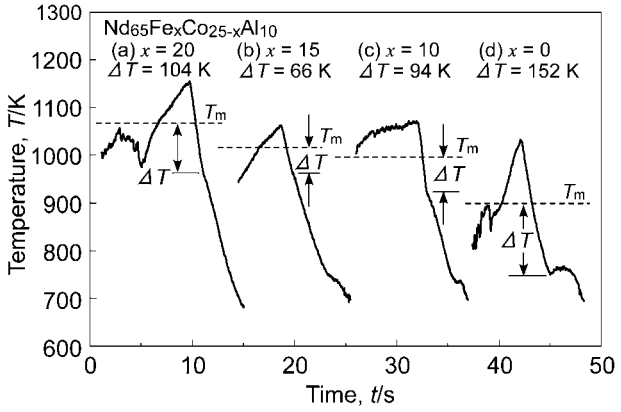

Fig. 1 Typical cooling curves of $Nd_{65}Fe_xCo_{25-x}Al_{10}$ samples by the gas jet flow type electromagnetic levitation. The broken lines are the melting temperature T_m.

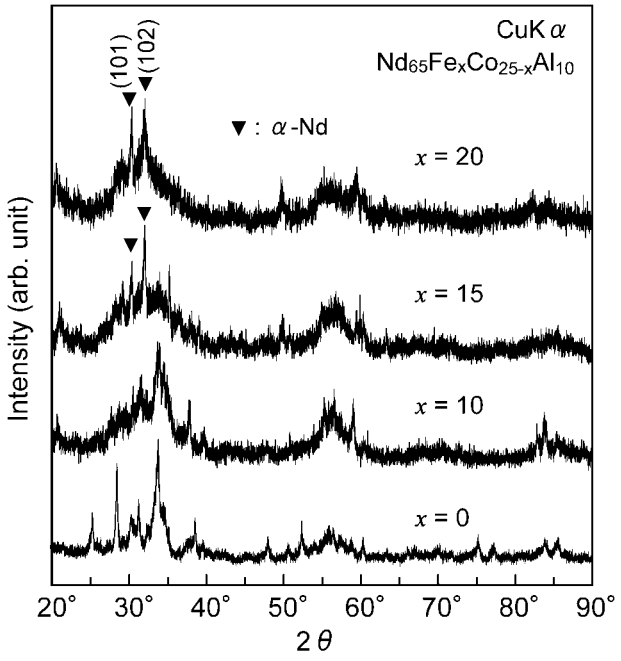

Fig. 2 XRD patterns of $Nd_{65}Fe_xCo_{25-x}Al_{10}$ samples by the gas jet flow type electromagnetic levitation.

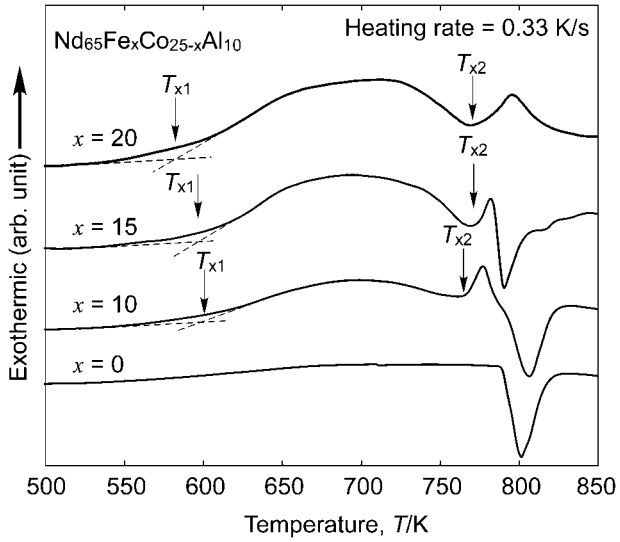

Fig. 3 DTA curves of $Nd_{65}Fe_xCo_{25-x}Al_{10}$ samples by the gas jet flow type electromagnetic levitation.

start to the detection limit for pyrometer) are approximately 100 and 60 K/s, respectively. Then, the undercooling ΔT, defined as the melting temperature minus the nucleation temperature of primary crystal, showed high values as 66–152 K. The ratio of the undercooing ΔT and the melting temperature T_m, $\Delta T/T_m$, is 0.06–0.17. The undercooling degree and the ratio of undercooling and melting temperature of the $Nd_{65}Co_{25}Al_{10}$ sample is the highest value of them all.

3.2 Amorphous phase formation

Figure 2 shows the XRD patterns of the samples corresponding to Fig. 1. As can be seen, the XRD patterns for Nd-Fe-Co-Al samples reveal the characteristic broad diffraction peaks typical of an amorphous structure. But then α-Nd peaks or crystal phase were detected in XRD pattern, too. Though the undercooling of $Nd_{65}Co_{25}Al_{10}$ in the cooling curves is the largest value of them all, the crystalline phases are predominant in the XRD pattern. Figure 3 shows the DTA curves of $Nd_{65}Fe_xCo_{25-x}Al_{10}$ ($x = 0$, 10, 15 and 20) samples obtained during continuous heating with 0.33 K/s. Two exothermic peaks were observed in DTA curves of $x = 10$, 15 and 20. However, the glass transition temperature wasn't detected in the DTA curves. The low temperature exothermic event has broad peak, and the onset temperature of exothermic peak is 581, 597, 600 K for $x = 20$, 15 and 10, respectively. The exothermic peak in the higher temperature region is 770, 771 and 765 K for $x = 20$, 15 and 10, respectively. These exothermic peaks correspond to the massive crystallization of amorphous phase. Also, in $x = 10$ and 15, the endothermic heat flow event is observed in the immediate aftermath of the exothermic peak. These behaviors, the endothermic peak in the immediate aftermath of the exothermic peak, agree well with previously published results on Nd-based amorphous alloys.[4,7] In published results, the broad exothermic peak was attributed to an early crystallization or growth of crystalline phases. In this study, in order to elucidate the broad exothermic peak, the DTA measurement was carried out repeatedly. All the exothermic peaks are irreversible reaction, as each of them disappears in a second heating run. This indicates that $Nd_{65}Fe_xCo_{25-x}Al_{10}$ ($x = 10$, 15 and 20) samples formed the amorphous phase. It is suggested that this broad peak indicates an exothermic reaction due to the structure relaxation depending on the local atomic arrangement transformation in the amorphous phase. Also, the cooling curves, XRD patterns and DTA curves similar to the $Nd_{65}Fe_xCo_{25-x}Al_{10}$ ($x = 10$, 15 and 20) samples was shown as for those of $Nd_{60}Fe_xCo_{30-x}Al_{10}$ ($x = 10$, 15 and 20) samples.[7,9] Those of $Nd_{55}Fe_xCo_{35-x}Al_{10}$ ($x = 10$, 15 and 20) samples, however, were not similar to those of two series of alloys. The $Nd_{55}Fe_xCo_{35-x}Al_{10}$ samples have low undercooling level and the crystalline phases were predominant in the XRD patterns (not shown). However, the undercooling level in all samples is not high in order to form the fully amorphous alloy. Also, Nd-Fe-Co-Al alloys tend to solidify in a metastable state (*e.g.* amorphous state).[4] This may be

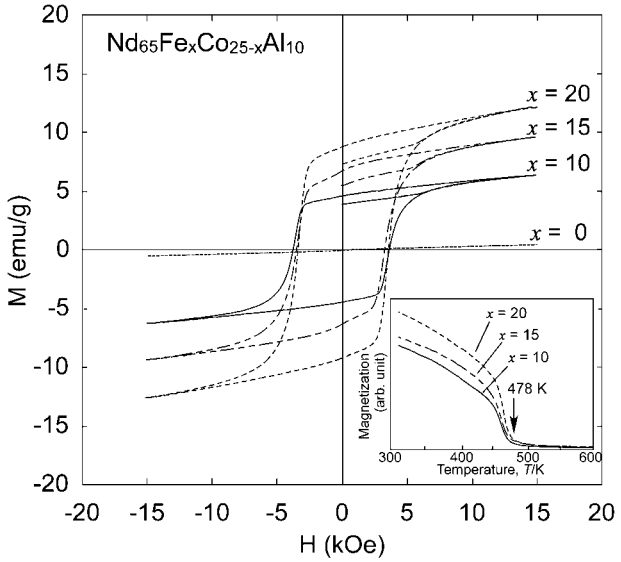

Fig. 4 M-H loops of $Nd_{65}Fe_xCo_{25-x}Al_{10}$ samples by the gas jet flow type electromagnetic levitation. The inset shows the thermomagnetic curves for $Nd_{65}Fe_xCo_{25-x}Al_{10}$ samples. The Curie temperature T_c was defined as the point of intersection between the linearly extrapolated curves of ferromagnetic and paramagnetic temperature region in this study.

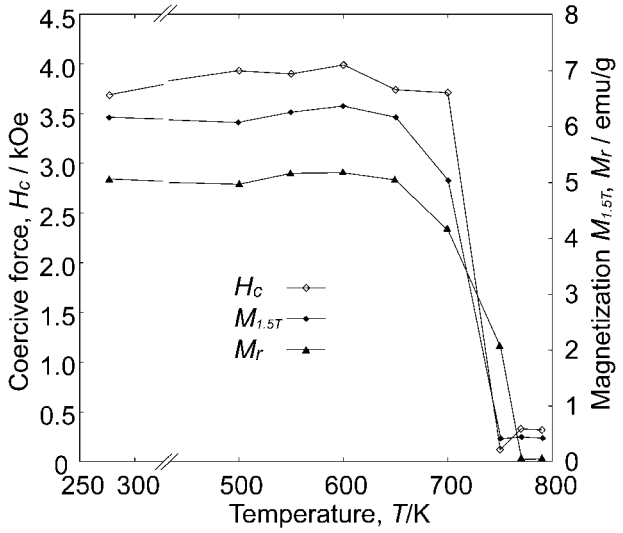

Fig. 5 Dependence of H_c, $M_{1.5\,T}$ and M_r on isothermal annealing temperature for $Nd_{65}Fe_{10}Co_{15}Al_{10}$ alloy (annealing for 60 min).

one of the reasons for amorphous phase formation by the gas jet flow type levitating process.

3.3 Magnetic properties

Figure 4 shows the M-H hysteresis loops of the solidified $Nd_{65}Fe_xCo_{25-x}Al_{10}$ samples, which were measured at room temperature with a maximum applied field of 1.5 T. The $Nd_{65}Fe_xCo_{25-x}Al_{10}$ ($x = 10$, 15 and 20) samples exhibit large coercivity values of 3.5–3.7 kOe. The substituting Co for Fe is increased the coercivity value. The Curie temperature exhibits 478 K in all samples (see inset in Fig. 4). It suggests the presence of the same magnetic phase with a similar microstructure in alloys with different composition. We have previously reported that the exchange coupling between Nd atom and Fe atom was enhanced by Co addition in $Nd_{60}Fe_xCo_{30-x}Al_{10}$ ($x = 10$, 15 and 20) samples. Furthermore, by increasing the substituting Co for Fe, the random magnetic anisotropy was increased because of the exchange coupling of Nd-Co.[7,12] Thereby, the coercivity value of $Nd_{65}Fe_{10}Co_{15}Al_{10}$ sample is the largest value. Also, the M-H loops are not saturated. This behavior may depend on the volume fraction of the amorphous phase.

The thermal stability of the hard magnetic properties is examined by isothermal annealing of the solidified samples. The $Nd_{65}Fe_{10}Co_{15}Al_{10}$ sample was chosen for isothermal annealing experiments due to the highest coercivity force in the Nd-based alloys. The sample was heated at 20 K/min to the annealing temperatures and annealed for 60 min. Figure 5 shows the dependence of coercivity H_c, maximum magnetization at 1.5 T $M_{1.5\,T}$ and remanence M_r on various isothermal annealing temperatures for the $Nd_{65}Fe_{10}Co_{15}Al_{10}$ sample. The hard magnetic properties remain almost unchanged in the annealing temperature range from room temperature up to 700 K. The coercivity force increases slightly from room temperature to 600 K and then is 4 kOe. And then the coercivity value decrease slightly up to 3.7 kOe at 700 K and then decrease drastically up to 0.1 kOe at 750 K. It is suggested that the coercivity value annealed at 770 K increases slightly due to heating more than eutectic temperature. The temperature for decreasing of coercivity from 600 K corresponds to the first crystallization temperature T_{x1}. The high coercivity may be related to the amorphous phase. Also, the $Nd_{55}Fe_xCo_{35-x}Al_{10}$ ($x = 10$, 15 and 20) alloys consisting of crystalline have low coercivity value, 0.09–1.33 kOe (not shown).

4. Conclusion

By the gas jet flow type electromagnetic levitation, which enables to solidify the levitated melt in the containerless state, the bulk amorphous formation and high coercivity appearance were examined and then we obtained the following results.

(1) In containerless process, Nd-Fe-Co-Al samples exhibited to form an amorphous phase and amorphous formation ability depends on the Nd or Fe content. Also, the validity for metastable phase formation of gas jet flow type levitating process was clarified.
(2) The coercivity value increases with Co content, but the amorphous formation ability decrease.
(3) The hard magnetic properties are stable in the annealing temperature range from room temperature to 700 K.

Acknowledgements

This work has been supported by a Grant-in-Aid for Scientific Research (C)(2), No. 15560646 from The Ministry of Education, Culture, Sports, Science and Technology.

REFERENCES

1) A. Takeuchi and A. Inoue: Mater. Trans. **43** (2002) 1985–1991.
2) X. Z. Wang, Y. Li, J. Ding, L. Si and H. Z. Kong: J. Alloys. Comp. **290** (1999) 209–215.

3) M. X. Pan, B. C. Wei, L. Xia, W. H. Wang, D. Q. Zhao, Z. Zhang and B. S. Han: Intermetallics **10** (2002) 1215–1219.
4) B. C. Wei, W. Löser, L. Xia, S. Roth, M. X. Pan, W. H. Wang and J. Eckert: Acta Mater. **50** (2002) 4357–4367.
5) G. Kumar, J. Eckert, S. Roth, W. Löser, L. Schultz and S. Ram: Acta Mater. **51** (2003) 229–238.
6) G. Kumar, J. Eckert, S. Roth, W. Löser, K-H. Müller and L. Schultz: Mater. Sci. Eng. **A375–377** (2004) 1083–1086.
7) S. Azumo, S. Utsuno and K. Nagayama: Mater. Trans., JIM **47** (2006) 1568–1571.
8) A. Inoue, T. Zhang, A. Takeuchi and W. Zhang: Mater. Trans., JIM **37** (1996) 636–640.
9) S. Azumo, S. Utsuno and K. Nagayama: J. Japan Inst. Metals **70** (2006) 138–141.
10) H. Yasuda, I. Ohanaka, Y. Ninomiya, R. Ishii, S. Fujita and K. Kishio: J. Crystal Growth **260** (2004) 475–485.
11) H. Yasuda, Y. Tamura, Y. Nagira, I. Ohnaka, Y. Yokoyama and A. Inoue: Mater. Trans. **46** (2005) 2762–2767.
12) K. Nagayama, H. Ino, N. Saito, Y. Nakagawa, E. Kita and K. Siratori: J. Phys. Soc. Jpn. **59** (1990) 2483.